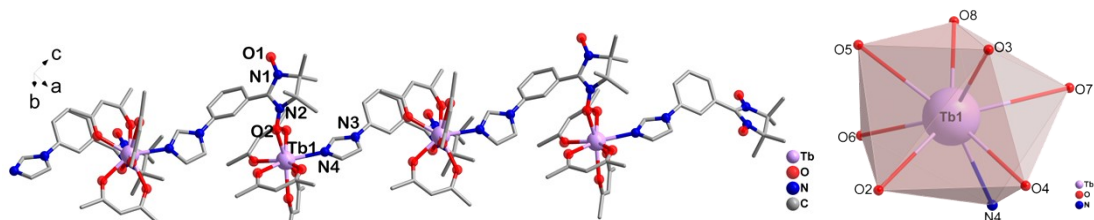


## Slow magnetic relaxation and selective luminescent sensor of Ln-radical chain involving imidazole-substituted nitronyl nitroxide radical

Qing Zhong,<sup>a</sup> Huiyang Dong,<sup>a</sup> Yi Liu<sup>a</sup> and Mei Zhu<sup>\*a</sup>

<sup>a</sup>Department of Chemistry, Key Laboratory of Surface & Interface Science of Polymer Materials of Zhejiang Province, Zhejiang Sci-Tech University, Hangzhou, 310018, China



**Fig. S1** (left) Crystal structure of complex 2 (All hydrogen and fluorine atoms are omitted for clarity) and coordination polyhedron of Tb (right).

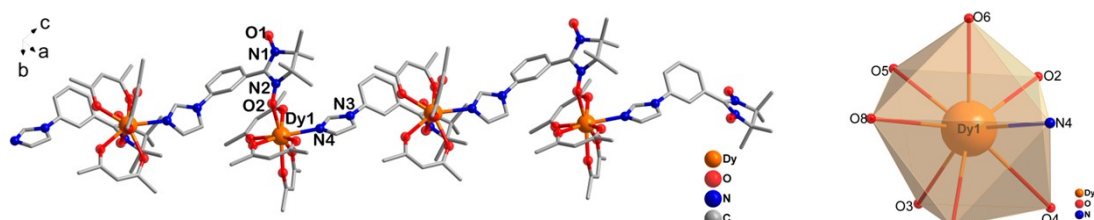


**Fig. S2** (left) Crystal structure of complex 3 (All hydrogen and fluorine atoms are omitted for clarity) and coordination polyhedron of Dy (right).

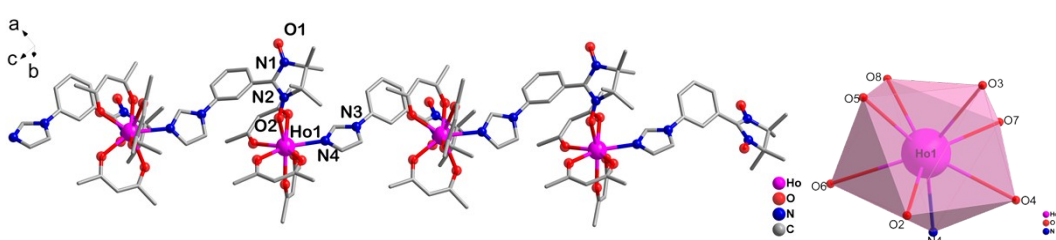


**Fig. S3** (left) Crystal structure of complex 4 (All hydrogen and fluorine atoms are omitted for clarity) and coordination polyhedron of Ho(right).

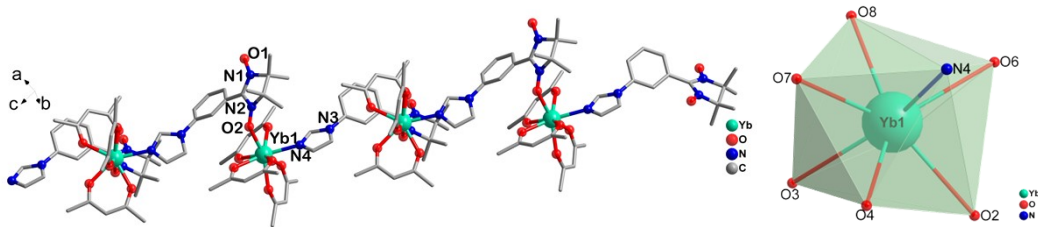


**Fig. S4** (left) Crystal structure of complex **5** (All hydrogen and fluorine atoms are omitted for clarity) and coordination polyhedron of Yb (right).

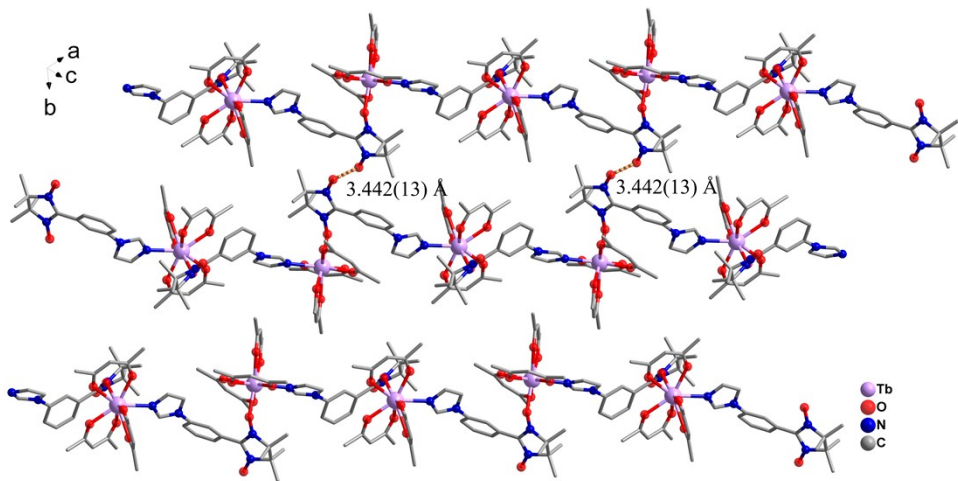


**Fig. S5** Crystal packing diagram of complex **2** (All F and some H atoms are omitted for clarity).

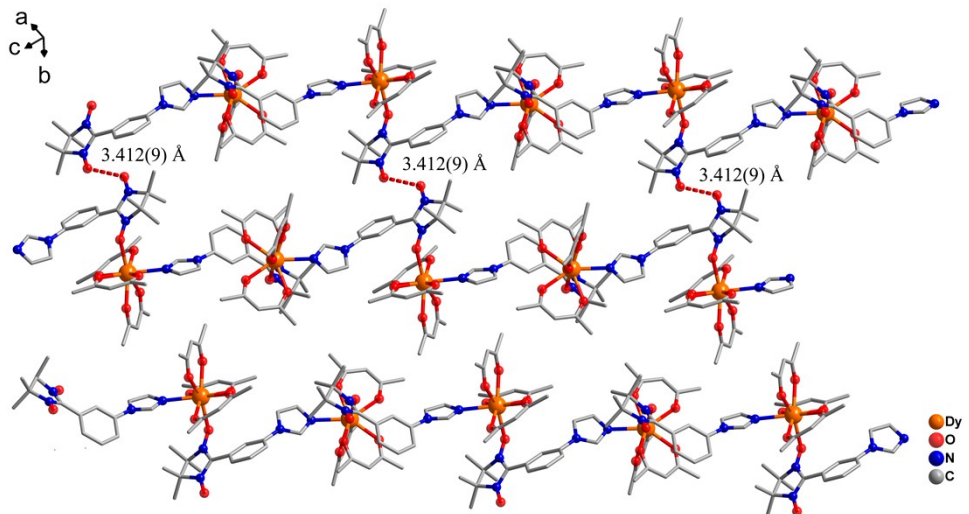


**Fig. S6** Crystal packing diagram of complex **3** (All F and some H atoms are omitted for clarity).

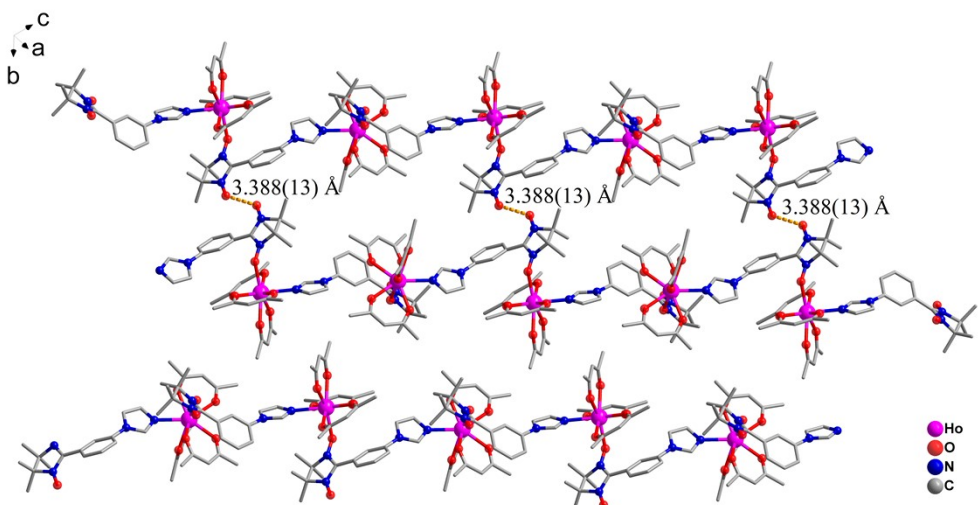


**Fig. S7** Crystal packing diagram of complex 4 (All F and some H atoms are omitted for clarity).

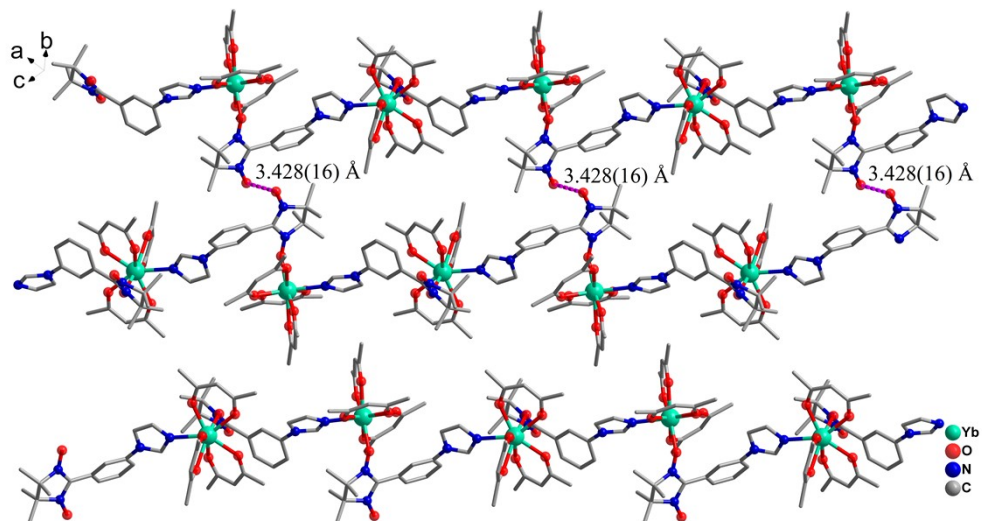


**Fig. S8** Crystal packing diagram of complex 5 (All F and some H atoms are omitted for clarity).

**Table S1.** Selected bond lengths ( $\text{\AA}$ ) and angles ( $^\circ$ ) for complex 1.

Bonds			
$\text{Gd}(1)\text{--O}(2)$	2.388(6)	$\text{Gd}(1)\text{--O}(3)$	2.403(5)
$\text{Gd}(1)\text{--O}(4)$	2.365(6)	$\text{Gd}(1)\text{--O}(5)$	2.351(5)
$\text{Gd}(1)\text{--O}(6)$	2.379(5)	$\text{Gd}(1)\text{--O}(7)$	2.369(5)
$\text{Gd}(1)\text{--O}(8)$	2.425(5)	$\text{Gd}(1)\text{--N}(4)$	2.496(6)
$\text{N}(1)\text{--O}(1)$	1.274(8)	$\text{N}(2)\text{--O}(2)$	1.323(8)

<i>Angles</i>			
O(2)-Gd(1)-O(3)	76.10(17)	O(2)-Gd(1)-O(4)	78.85(19)
O(2)-Gd(1)-O(5)	96.24(19)	O(2)-Gd(1)-O(6)	74.18(16)
O(2)-Gd(1)-O(7)	145.27(17)	O(2)-Gd(1)-O(8)	144.78(16)
O(2)-Gd(1)-N(4)	96.85(18)	O(3)-Gd(1)-O(4)	72.59(18)
O(3)-Gd(1)-O(5)	72.38(17)	O(3)-Gd(1)-O(6)	130.49(17)
O(3)-Gd(1)-O(7)	74.20(19)	O(3)-Gd(1)-O(8)	129.89(18)
O(3)-Gd(1)-N(4)	146.04(19)	O(4)-Gd(1)-O(5)	144.77(18)
O(4)-Gd(1)-O(6)	136.45(19)	O(4)-Gd(1)-O(7)	75.4(2)
O(4)-Gd(1)-O(8)	127.47(19)	O(4)-Gd(1)-N(4)	73.5(2)
O(5)-Gd(1)-O(6)	72.57(18)	O(5)-Gd(1)-O(7)	91.6(2)
O(5)-Gd(1)-O(8)	74.90(18)	O(5)-Gd(1)-N(4)	141.53(19)
O(6)-Gd(1)-O(7)	70.64(16)	O(6)-Gd(1)-O(8)	70.64(16)
O(6)-Gd(1)-N(4)	76.54(19)	O(7)-Gd(1)-O(8)	69.86(18)
O(7)-Gd(1)-N(4)	97.8(2)	O(8)-Gd(1)-N(4)	73.61(18)
Gd(1)-O(2)-N(2)	134.8(4)		

**Table S2.** Selected bond lengths ( $\text{\AA}$ ) and angles ( $^\circ$ ) for complex **2**.

<i>Bonds</i>			
Tb(1)-O(2)	2.377(4)	Tb(1)-O(3)	2.337(4)
Tb(1)-O(4)	2.359(4)	Tb(1)-O(5)	2.377(4)
Tb(1)-O(6)	2.350(4)	Tb(1)-O(7)	2.412(4)
Tb(1)-O(8)	2.343(4)	Tb(1)-N(4)	2.495(5)
N(1)-O(1)	1.263(6)	N(2)-O(2)	1.320(6)

<i>Angles</i>			
O(2)-Tb(1)-O(3)	96.27(15)	O(2)-Tb(1)-O(4)	74.41(13)

O(2)-Tb(1)-O(5)	75.73(14)	O(2)-Tb(1)-O(6)	78.50(15)
O(2)-Tb(1)-O(7)	144.81(14)	O(2)-Tb(1)-O(8)	144.71(14)
O(2)-Tb(1)-N(4)	96.74(14)	O(3)-Tb(1)-O(4)	72.62(15)
O(3)-Tb(1)-O(5)	72.35(14)	O(3)-Tb(1)-O(6)	144.77(15)
O(3)-Tb(1)-O(7)	75.02(15)	O(3)-Tb(1)-O(8)	91.71(16)
O(3)-Tb(1)-N(4)	141.73(15)	O(4)-Tb(1)-O(5)	130.39(14)
O(4)-Tb(1)-O(6)	136.28(15)	O(4)-Tb(1)-O(7)	70.45(13)
O(4)-Tb(1)-O(8)	140.38(14)	O(4)-Tb(1)-N(4)	76.56(15)
O(5)-Tb(1)-O(6)	72.61(14)	O(5)-Tb(1)-O(7)	130.25(14)
O(5)-Tb(1)-O(8)	74.11(15)	O(5)-Tb(1)-N(4)	145.88(14)
O(6)-Tb(1)-O(7)	127.65(15)	O(6)-Tb(1)-O(8)	75.34(16)
O(6)-Tb(1)-N(4)	73.28(16)	O(7)-Tb(1)-O(8)	70.40(15)
O(7)-Tb(1)-N(4)	73.67(15)	O(8)-Tb(1)-N(4)	97.96(16)
Tb(1)-O(2)-N(2)	133.7(3)		

**Table S3.** Selected bond lengths ( $\text{\AA}$ ) and angles ( $^\circ$ ) for complex **3**.

<i>Bonds</i>			
Dy(1)–O(2)	2.364(4)	Dy(1)–O(3)	2.332(4)
Dy(1)–O(4)	2.353(4)	Dy(1)–O(5)	2.368(4)
Dy(1)–O(6)	2.336(4)	Dy(1)–O(7)	2.376(4)
Dy(1)–O(8)	2.331(4)	Dy(1)–N(4)	2.494(4)
N(1)–O(1)	1.261(6)	N(2)–O(2)	1.306(6)
<i>Angles</i>			
O(2)-Dy(1)-O(3)	96.34(14)	O(2)-Dy(1)-O(4)	73.78(13)
O(2)-Dy(1)-O(5)	75.89(14)	O(2)-Dy(1)-O(6)	78.88(14)

O(2)-Dy(1)-O(7)	144.53(14)	O(2)-Dy(1)-O(8)	144.69(14)
O(2)-Dy(1)-N(4)	96.55(14)	O(3)-Dy(1)-O(4)	73.25(14)
O(3)-Dy(1)-O(5)	71.64(14)	O(3)-Dy(1)-O(6)	144.51(14)
O(3)-Dy(1)-O(7)	74.86(14)	O(3)-Dy(1)-O(8)	91.09(15)
O(3)-Dy(1)-N(4)	141.98(14)	O(4)-Dy(1)-O(5)	129.95(13)
O(4)-Dy(1)-O(6)	135.98(14)	O(4)-Dy(1)-O(7)	70.78(13)
O(4)-Dy(1)-O(8)	140.97(14)	O(4)-Dy(1)-N(4)	76.34(14)
O(5)-Dy(1)-O(6)	73.11(14)	O(5)-Dy(1)-O(7)	129.92(14)
O(5)-Dy(1)-O(8)	73.86(14)	O(5)-Dy(1)-N(4)	146.34(15)
O(6)-Dy(1)-O(7)	127.67(15)	O(6)-Dy(1)-O(8)	75.27(15)
O(6)-Dy(1)-N(4)	73.25(15)	O(7)-Dy(1)-O(8)	70.66(14)
O(7)-Dy(1)-N(4)	73.94(14)	O(8)-Dy(1)-N(4)	98.55(15)
Dy(1)-O(2)-N(2)	134.3(3)		

**Table S4.** Selected bond lengths ( $\text{\AA}$ ) and angles ( $^\circ$ ) for complex **4**.

<i>Bonds</i>			
Ho(1)–O(2)	2.360(4)	Ho(1)–O(3)	2.318(4)
Ho(1)–O(4)	2.354(4)	Ho(1)–O(5)	2.362(4)
Ho(1)–O(6)	2.322(4)	Ho(1)–O(7)	2.372(4)
Ho(1)–O(8)	2.328(4)	Ho(1)–N(4)	2.480(5)
N(1)–O(1)	1.252(6)	N(2)–O(2)	1.303(6)
<i>Angles</i>			
O(2)-Ho(1)-O(3)	96.43(15)	O(2)-Ho(1)-O(4)	73.81(14)
O(2)-Ho(1)-O(5)	75.65(14)	O(2)-Ho(1)-O(6)	78.78(15)
O(2)-Ho(1)-O(7)	144.45(14)	O(2)-Ho(1)-O(8)	144.48(14)

O(2)-Ho(1)-N(4)	96.74(15)	O(3)-Ho(1)-O(4)	73.34(14)
O(3)-Ho(1)-O(5)	71.47(14)	O(3)-Ho(1)-O(6)	144.54(14)
O(3)-Ho(1)-O(7)	74.85(15)	O(3)-Ho(1)-O(8)	90.86(16)
O(3)-Ho(1)-N(4)	142.21(15)	O(4)-Ho(1)-O(5)	129.67(14)
O(4)-Ho(1)-O(6)	135.87(15)	O(4)-Ho(1)-O(7)	70.67(14)
O(4)-Ho(1)-O(8)	141.10(15)	O(4)-Ho(1)-N(4)	76.65(15)
O(5)-Ho(1)-O(6)	73.33(15)	O(5)-Ho(1)-O(7)	130.13(15)
O(5)-Ho(1)-O(8)	73.89(15)	O(5)-Ho(1)-N(4)	146.27(16)
O(6)-Ho(1)-O(7)	127.74(16)	O(6)-Ho(1)-O(8)	75.36(16)
O(6)-Ho(1)-N(4)	72.96(15)	O(7)-Ho(1)-O(8)	70.94(15)
O(7)-Ho(1)-N(4)	73.90(15)	O(8)-Ho(1)-N(4)	98.48(16)
Ho(1)-O(2)-N(2)	133.7(3)		

**Table S5.** Selected bond lengths ( $\text{\AA}$ ) and angles ( $^\circ$ ) for complex **5**.

<i>Bonds</i>			
Yb(1)–O(2)	2.317(3)	Yb(1)–O(3)	2.284(3)
Yb(1)–O(4)	2.303(3)	Yb(1)–O(5)	2.332(3)
Yb(1)–O(6)	2.289(3)	Yb(1)–O(7)	2.352(3)
Yb(1)–O(8)	2.290(3)	Yb(1)–N(4)	2.440(3)
N(1)–O(1)	1.264(5)	N(2)–O(2)	1.309(5)
<i>Angles</i>			
O(2)-Yb(1)-O(3)	97.14(11)	O(2)-Yb(1)-O(4)	74.17(10)
O(2)-Yb(1)-O(5)	75.23(11)	O(2)-Yb(1)-O(6)	77.41(11)
O(2)-Yb(1)-O(7)	144.89(11)	O(2)-Yb(1)-O(8)	143.55(11)
O(2)-Yb(1)-N(4)	97.45(11)	O(3)-Yb(1)-O(4)	74.34(11)

O(3)-Yb(1)-O(5)	70.78(11)	O(3)-Yb(1)-O(6)	144.43(11)
O(3)-Yb(1)-O(7)	74.71(11)	O(3)-Yb(1)-O(8)	91.49(12)
O(3)-Yb(1)-N(4)	142.50(11)	O(4)-Yb(1)-O(5)	129.50(10)
O(4)-Yb(1)-O(6)	134.65(11)	O(4)-Yb(1)-O(7)	70.74(10)
O(4)-Yb(1)-O(8)	141.97(11)	O(4)-Yb(1)-N(4)	76.78(11)
O(5)-Yb(1)-O(6)	73.88(11)	O(5)-Yb(1)-O(7)	130.03(11)
O(5)-Yb(1)-O(8)	74.41(11)	O(5)-Yb(1)-N(4)	146.59(11)
O(6)-Yb(1)-O(7)	128.45(11)	O(6)-Yb(1)-O(8)	75.17(12)
O(6)-Yb(1)-N(4)	72.71(11)	O(7)-Yb(1)-O(8)	71.51(11)
O(7)-Yb(1)-N(4)	73.52(11)	O(8)-Yb(1)-N(4)	96.85(12)
Yb(1)-O(2)-N(2)	134.1(3)		

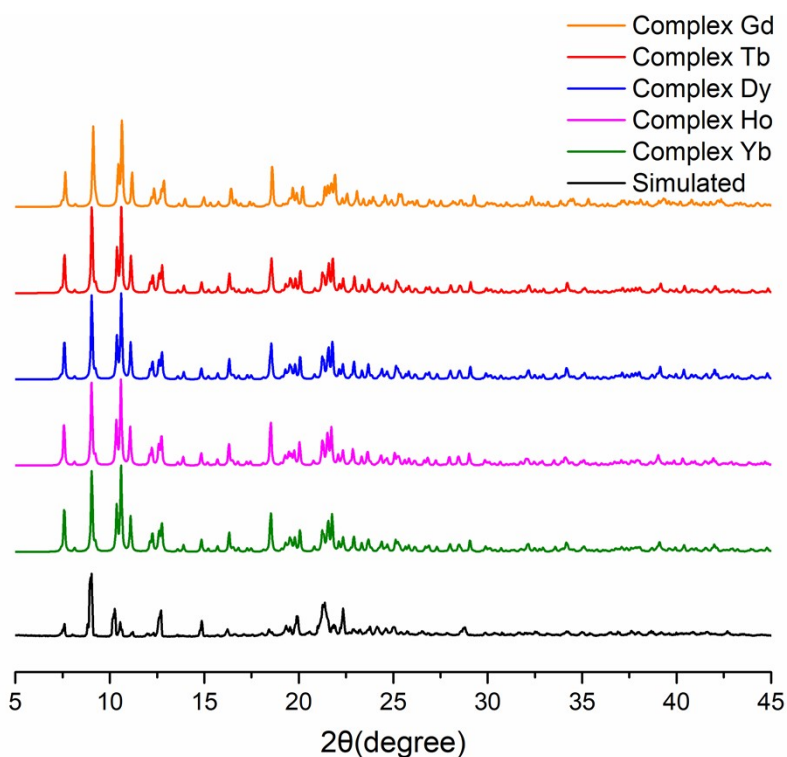


**Fig. S9** Powder X-ray diffraction patterns of complexes **1-5**.

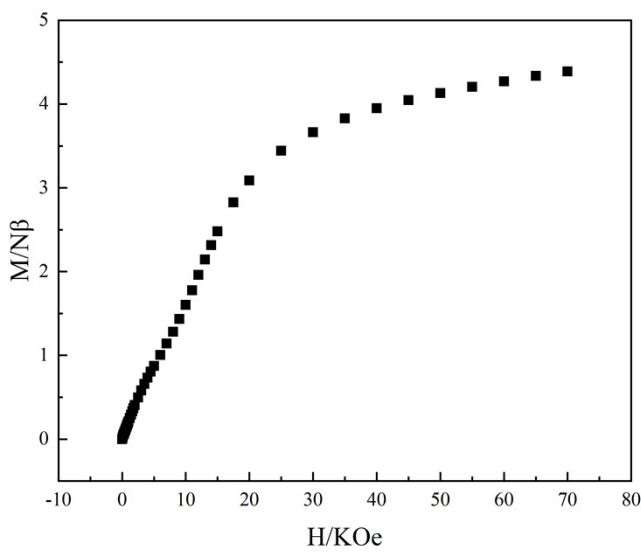


**Fig. S10** The  $M$  vs.  $H$  plots of complex **2** at 2.0 K.

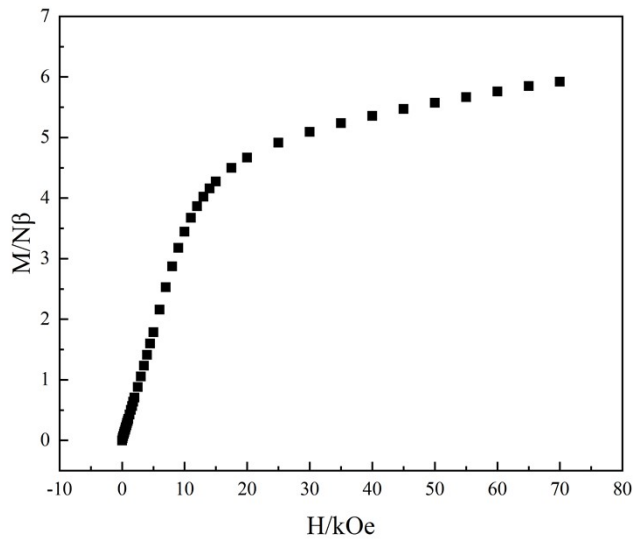


**Fig. S11** The  $M$  vs.  $H$  plots of complex **3** at 2.0 K.

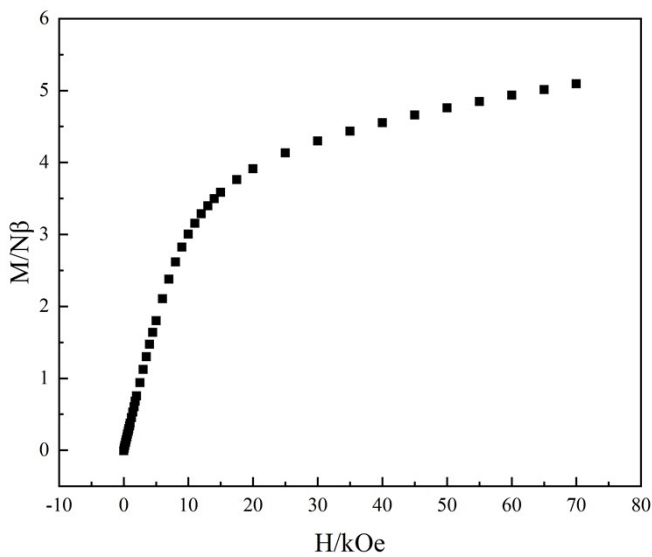


**Fig. S12** The  $M$  vs.  $H$  plots of complex **4** at 2.0 K.

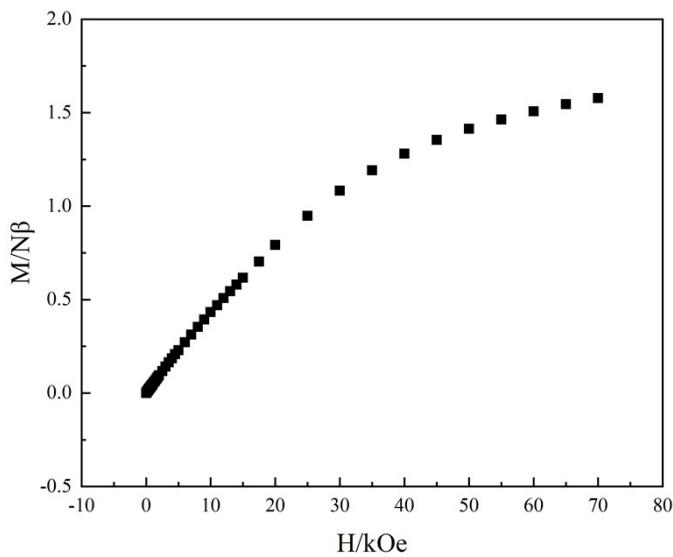


**Fig. S13** The  $M$  vs.  $H$  plots of complex **5** at 2.0 K.

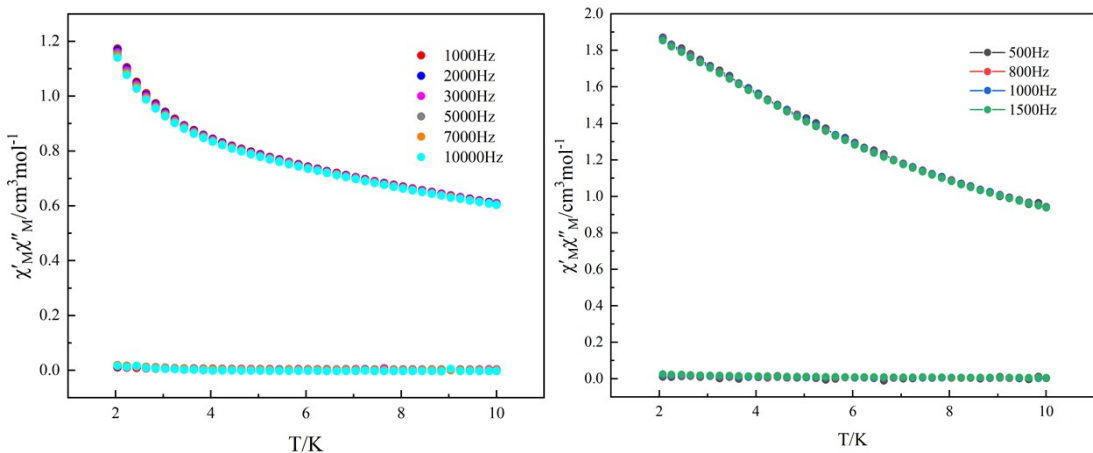


**Fig. S14** Temperature dependence of the in-phase and out-of-phase components of the ac magnetic susceptibility for complex **2** (left) and **3** (right) in zero dc fields.

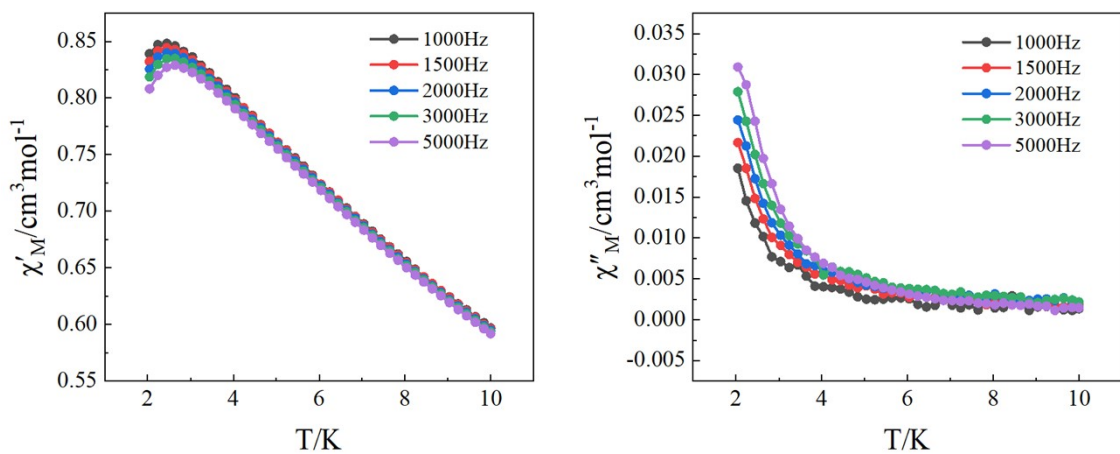


**Fig. S15** Temperature-dependent ac signals for **2** at a 3000 Oe dc field.

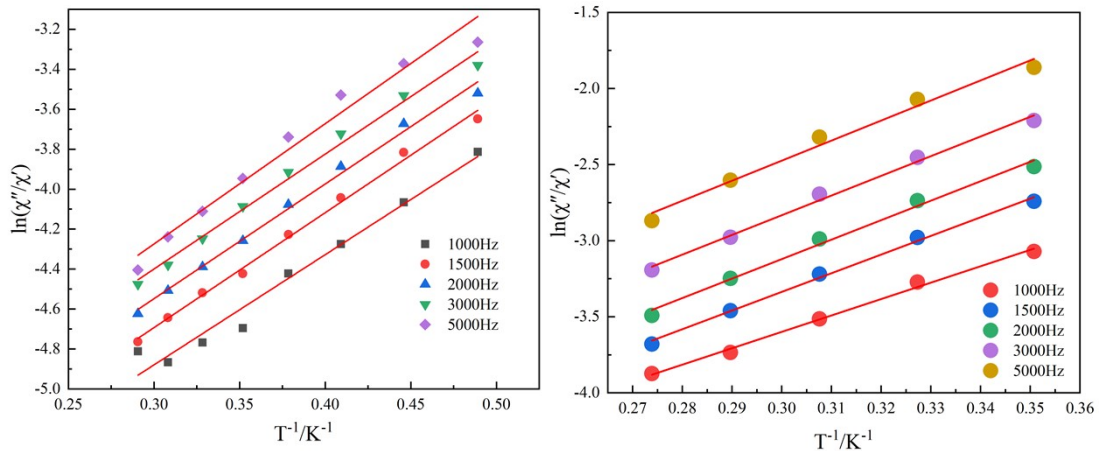


**Fig. S16** Extractive  $\ln(\chi''/\chi')$  vs  $1/T$  plot for **2** (left) and **3** (right) (solid-lines: fitting curves).

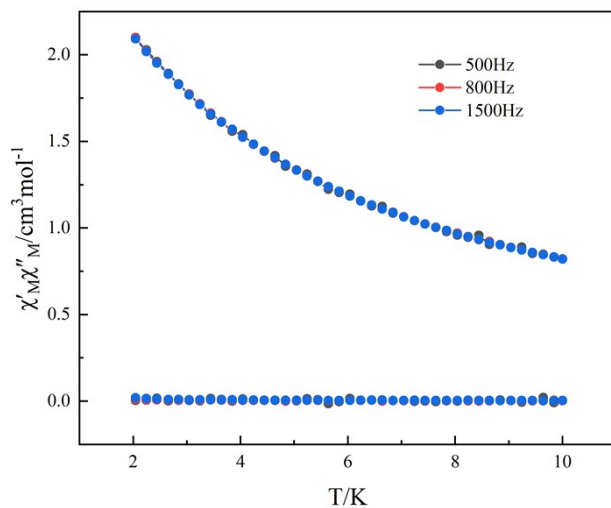


**Fig. S17** Temperature dependence of the in-phase and out-of-phase components of the ac magnetic susceptibility for complex **4**.

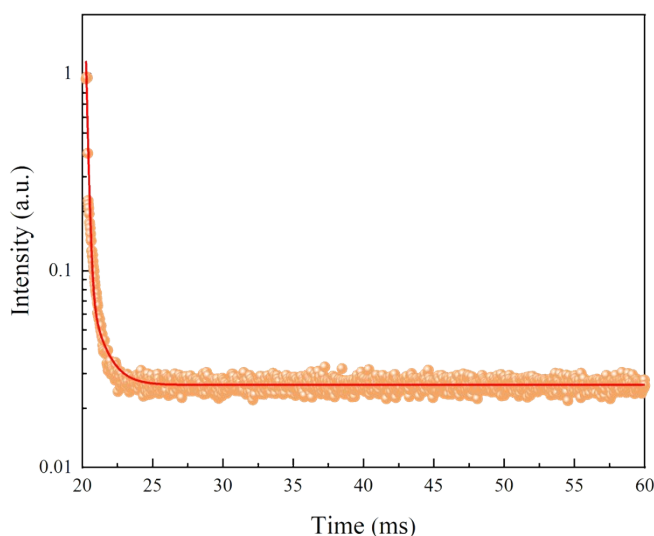


**Fig. S18** The fluorescence decay of complex **2** (solid-lines: fitting curves).

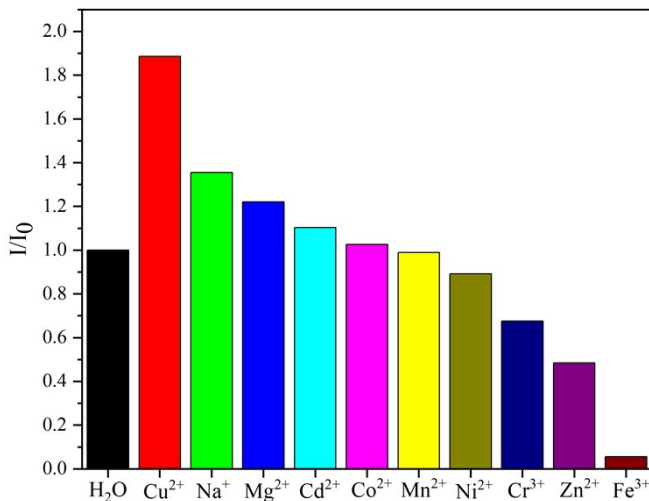


**Fig. S19** Luminescence intensity of the transition (543 nm) of complex **2** in different cations salt solution (1 mM).  $I$  and  $I_0$  denote the fluorescence intensity of complex **2** in cation solution and water, respectively.

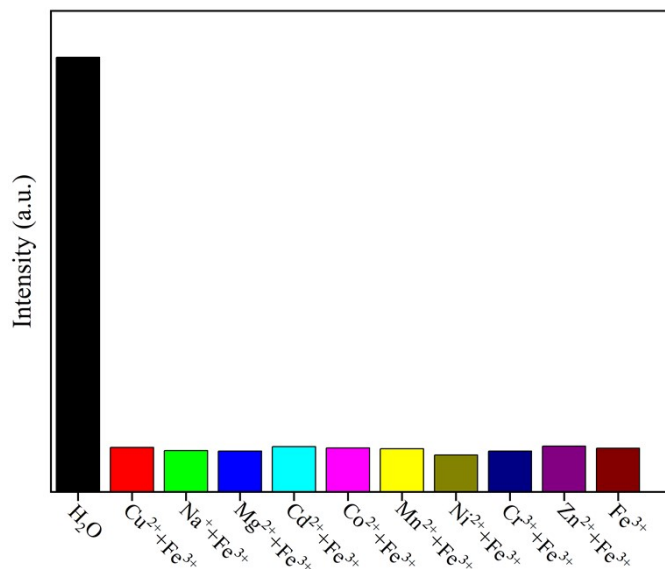


**Fig. S20** Comparison of the luminescence intensity of **2** in the presence of mixed cations.

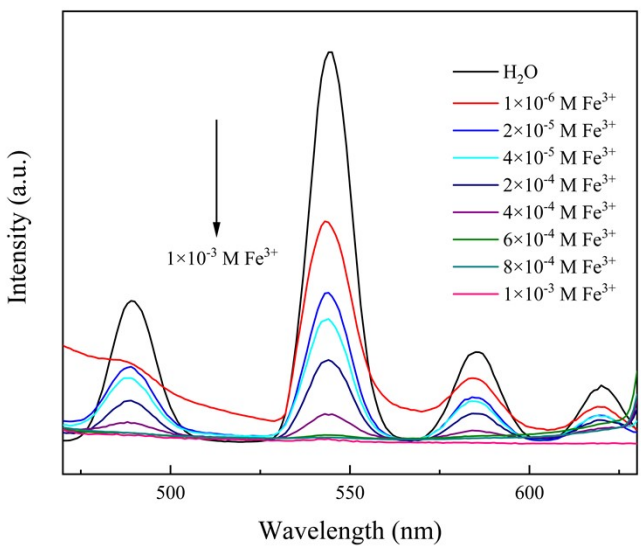


**Fig. S21** Emission spectra of complex **2** with different concentration of  $\text{Fe}^{3+}$  aqueous solution ( $\lambda_{\text{exc}} = 328 \text{ nm}$ ).

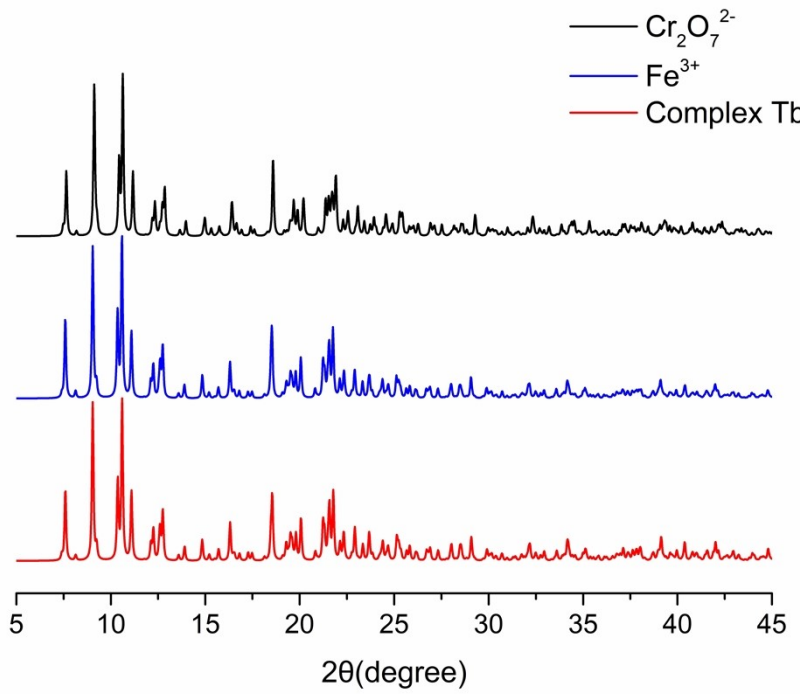


**Fig. S22** PXRD patterns of Tb complex after soaking in  $\text{Cr}_2\text{O}_7^{2-}$  and  $\text{Fe}^{3+}$  ions.

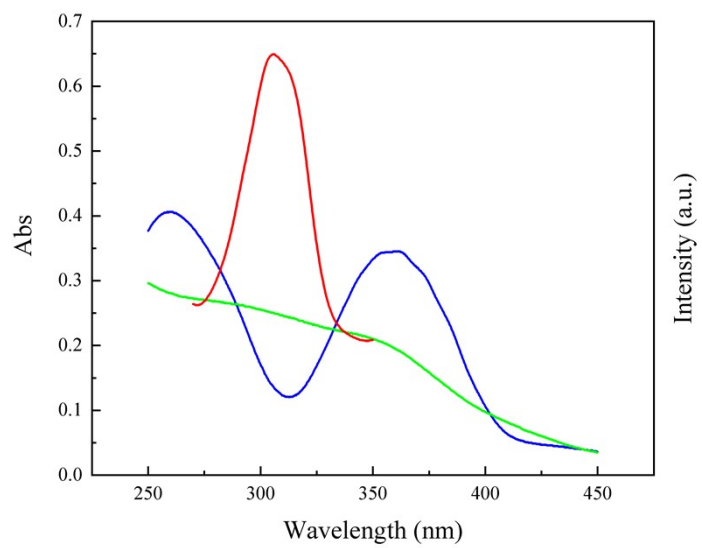


**Fig. S23** The UV-vis absorption spectra of  $\text{Cr}_2\text{O}_7^{2-}$  (blue) and  $\text{Fe}^{3+}$  (green), and the excitation spectra of complex **2** (red).